UDC 537.622 + 539.211:544.723 + 620.3 doi: 10.15407/hftp14.01.093

A.P. Kusyak [1], O.I. Oranska [1], D. Marcin Behunova [2], A.L. Petranovska [1], V.S. Chornyi [3], O.A. Bur'yanov [3], V.A. Dubok [4], P.P. Gorbyk [1]

XRD, EDX AND FTIR STUDY OF THE BIOACTIVITY OF 60S GLASS DOPED WITH La AND Y UNDER *IN VITRO* CONDITIONS

[1] Chuiko Institute of Surface Chemistry of National Academy of Sciences of Ukraine
17 General Naumov Str., Kyiv, 03164, Ukraine, E-mail: a_kusyak@ukr.net
[2] Institute of Geotechnics of Slovak Academy of Sciences
45 Watsonova Str., Kosice, 04001, Slovakia
[3] Bogomolets National Medical University
13 Taras Shevchenko Blvd., Kyiv, 01601, Ukraine
[4] Frantsevich Institute of Problems of Materials Science of National Academy of Sciences of Ukraine
3 Krzhyzhanovskoho Str., Kyiv, 03142, Ukraine

The aim of the work is the synthesis and study of the bioactivity of sol-gel glass (BG 60S) with molar composition 60 % SiO_2, 36 % CaO, 4 % P_2O_5 and samples doped with La and Y in vitro; studying their structural properties and changes upon contact with a model physiological environment (Kokubo's SBF), as well as justifying the possibility of their use for tissue regeneration and tissue engineering.

According to the results of research, the interaction of synthesized samples with SBF leads to a change in the phase composition and the ratio of amorphous and crystalline components. It is necessary to note long and intensive processes involving CO_3^{2-} ions for unalloyed and alloyed samples. The appearance of calcium carbonate in the form of vaterite with a simultaneous increase in the calcite content is one of the signs of high bioactivity of the synthesized samples. According to the results of XRD, EDX and FTIR studies after 28 days of soaking in SBF, the predominant surface elements are Ca and P in the composition of hydroxyapatite, and the elemental composition indicates active ion exchange processes according to the theory of bioactive glass dissolution in physiological fluids.

The change in the ratio of crystalline phases with the inclusion of mainly one crystalline phase of hydroxopatite within 28 days leads to a better structuredness of the surface of the synthesized samples and indicates that they have osteoconductive properties, can connect with bone tissue and have the appropriate biodegradation ability.

The results of the study indicate the promising nature of synthesized materials for tissue regeneration and tissue engineering.

***Keywords**: bioactive sol-gel glass, osteoconductivity, tissue regeneration, tissue engineering*

INTRODUCTION

Use of bone substitutes derived from biological products, such as demineralized bone matrix, platelet-rich plasma, hydroxyapatite, addition of growth factors (*e.g.*, bone morphogenetic protein) or synthetic, such as calcium sulfate, tricalcium phosphate ceramics, bioactive glass, or polymer-based substitutes are chosen as dependent on their purpose. The main limitation of the use of bone substitutes remains the treatment of large defects and the lack of vascularization in their central part.

Therefore, in the field of bone tissue engineering, the development of synthetic substitutes capable of maintaining rapid and extensive vascularization in their structure is a promising avenue of research [1].

Various types of bioactive glass synthesized by the sol-gel method have attracted the attention of researchers due to the convenience and versatility of the synthesis method. Bioactive glass is an ideal candidate for bone tissue engineering because it can bind to bone and stimulate bone cells to osteogenesis. The developed porous surface characteristic of sol-gel glass is a key factor to ensure cell migration into scaffolds, as well as *in vivo* vascularization and bone ingrowth. The presence of nano-sized pores can also provide additional functions to the scaffold, enhancing its bioactive properties and providing the capability to release drugs. Despite the achievements of application in biomedical fields, especially for the regeneration of bone tissue, and recent achievements allow the use for

soft tissues as well, the existing ones have been improved and new types of combinations of these materials are proposed [2–7].

Attention is focused on the chemical, surface, mechanical and biological properties, strategies for controlling the pore structure, shape, size and composition of bioactive sol-gel glass. It is assumed that the morphology and chemical composition of sol-gel bioactive glasses significantly affect their biological properties. Thus, the controlled synthesis of these materials is crucial for their effective use in biomedical fields [8–9].

One of the promising directions of biofunctionalization is the inclusion of cations or their mixture as modifiers of the silica matrix, which provides new properties, including antibacterial ones, without reducing the bioactivity of sol-gel glasses [10–21]. Such compositions are aimed at bone restoration therapy, antibacterial effect and prolonged action [22]. On the other hand, such biofunctionalization provides added value to the implant, as the graft not only fills and eliminates the defect, but also acts as a drug delivery system that locally supplies osteoregenerative agents.

This study describes the synthesis, methods, and research results of synthesized samples of 60S sol-gel glass and samples doped with La and Y: crystal structure, chemical composition, capability to form hydroxyapatite on the surface during interaction with a model physiological environment. The spectrum of therapeutic action of additives includes apoptosis of cancer cells, changes in the rate of resorption of bioceramics, selective immunomodulatory activity.

The results of the study indicate the promising nature of synthesized materials for tissue regeneration and tissue engineering.

EXPERIMENTAL PART

Research materials and methods. Sol-gel glass (60S) has a composition (mol.) of 60 % SiO_2, 36 % CaO, 4 % P_2O_5. The synthesis was carried out by sol-gel method using: tetraethyl orthosilicate (TEOS) $(C_2H_5O)_4Si$, triethyl phosphate (TEP) $(C_2H_5O)_3PO$, ethanol C_2H_5OH, calcium nitrate tetrahydrate $(Ca(NO_3)_2{\cdot}4H_2O)$, lanthanum(III) nitrate hexahydrate $(La(NO_3)_3{\cdot}6H_2O)$, yttrium(III) nitrate hexahydrate $(Y(NO_3)_3{\cdot}6H_2O)$, 59 % solution of nitric acid (HNO_3) (all reagents of qualification "chemically pure" (Merck Schuchardtohg (Germany)). Mass ratios of precursors for the synthesis of 60S glass were: $(C_2H_5O)_4Si$: $(C_2H_5O)_3PO$: $(Ca(NO_3)_2{\cdot}4H_2O)$: H_2O : C_2H_5OH = 8.59 : 1 : 5.85 : 9 : 3.

Preparation of sol-gel glass 60S. To obtain the sol-gel glass, the TEOS, TEP and ethanol are first poured into the above proportions, stirred on a magnetic stirrer for 30 min, and sonication was applied for 5 min. For hydration and getting sol added nitric acid, mixed again on the magnetic mixer for 30 min and again sonicated for 5 min. Separately prepared an aqueous solution of calcium nitrate, mixing the specified quantities of components on a magnetic stirrer for at least 10 min. Then a solution of calcium nitrate is added to the sol, stirred on a magnetic stirrer for at least 40 min, sonicated for 5 min and to complete the polycondensation processes withstand the sol for 24 h at room temperature and then heated in a sealed container in a dry oven for 24 h at 60 °C. The resulting gel is kept eat least 48 h at 120 °C and then slowly heated (at least 4 h) to 700 °C and calcined at this temperature for 2 h.

For the synthesis of doped La (or Y) sol-gel glass $Ca(NO_3)_2{\cdot}4H_2O$ was replaced by $La(NO_3)_3$ $6H_2O$ (or $Y(NO_3)_3{\cdot}6H_2O$) (in the ratio 6 : 4 (mol%)).

The produced glass was ground with a mortar and pestle to disagglomerate the particles.

For research *in vitro* apatite forming ability from the studied samples of sol-gel glasses (0.06+0.005 g), disks were formed (d = 13 mm, h = 280 μm, pressure 10 tons) for which the corresponding volume of SBF was calculated. Assessment of bioactivity was carried out using the standard *in vitro* procedure described by [23] and ISO23317:2014 using analytical reagent-grade chemicals NaCl, $NaHCO_3$, KCl, $K_2HPO_4{\cdot}3H_2O$, $MgCl_2{\cdot}6H_2O$, $CaCl_2$, trishydroxymethyl aminomethane [Tris-buffer, $(CH_2OH)_3CNH_2$], and 1 M HCl.

Characterisations of sol-gel glass 60S. The samples obtained were characterized by a scanning electron microscope MIRA 3 FE-SEM microscope (TESCAN, Czech Republic) equipped with an Energy-dispersive X-ray detector (EDX) Oxford Instruments, UK). EDX spectra of the prepared samples before and after immersion in SBF on days 7, 14 and 28 were

used to study changes in the elemental composition of the sample surface.

In vitro apatite forming ability. The bioactive glass samples, before and after immersion in SBF were examined by Fourier transform infrared spectroscopy (FTIR), thin-film X-ray diffraction and scanning electron microscopy after soaking for 7, 14 and 28 days respectively. Samples were immersed in SBF in clean plastic bottles, which had previously been washed using HCl and deionized water. The bottles were placed inside an thermostat at a controlled temperature of 36.5 °C. SBF solutions were updated during the immersion period every 24 h for all studies: measurement of XRD, EDX, FTIR. The samples were extracted from the SBF solution after given times of 7, 14 and 28 days. After immersion at 36.5 °C for different periods within 4 weeks in the SBF, the sample was take out from the SBF and wash it with deionized water. The specimen was dried at 90 °C and stored in a desiccator.

The volume of SBF that is used for testing calculated using the following Eq. 1 [23]:

$$V_s = S_a / 10, \quad (1)$$

where Vs is the volume of SBF (ml) and S_a is the apparent surface area (mm^2).

Infrared spectra were recorded on a FTIR Spectrometer Tensor 27 (Bruker Optik GmbH, Germany) in the range 4000–400 cm^{-1} using KBr pellets with a resolution of 2 cm^{-1}.

Structural studies of the obtained samples were performed by powder X-ray diffraction method (XRD) using a DRON-4-07 diffractometer with Ni filtered CuK_α radiation, the Bragg-Brentano focusing, in 2θ range of 10–80° with a step of 0.05°, exposure of 1 s. Phase identification was performed with PDF-2 database. The average crystal size was determined on the broadening of the corresponding most intense line according to the Scherrer equation.

RESULTS AND DISCUSSION

Fig. 1 shows the XRD diffractograms of the bioactive glass 60S before and after soaking in SBF solution for different time periods. On the diffractogram of the original glass 60S (Fig. 1 *a*), an asymmetric diffuse halo is observed in the area of diffraction angles, about 22°, which indicates the amorphous character of the synthesized sol-gel glass. The most intense crystalline peaks, which appear against the background of the halo, belong to the weakly crystalline phase of hydroxopatite $Ca_{10}(PO_4)_6(OH)_2$ (ICDD N 74-566) and calcite $CaCO_3$ (ICDD N 72-1937). That is, under the given synthesis conditions, 60S glass contains crystalline inclusions of at least two phases.

Soaking 60S glass in SBF leads to a change in its phase composition and the ratio of amorphous and crystalline components. Thus, after 7 days of soaking in SBF, peaks related to calcium carbonate in the form of vaterite (ICDD N 72-506) appear on the diffractogram of the sample with a simultaneous increase in the calcite content according to the increase in the intensity of its diffraction peaks.

The formation of vaterite, the least stable polymorph of $CaCO_3$, but stable enough to ensure the presence of a potential ionic buffer for bone regeneration and which has sufficient reactivity for conversion from $CaCO_3$ to hydroxyapatite (HA) [24] is one of the signs of high bioactivity of the synthesized samples. A decrease in the intensity of hydroxopatite peaks indicates a decrease in its content (Fig. 1 *b*).

After 14 days of soaking the glass in SBF, there is a decrease in the intensity of the vaterite peaks while the intensity of the calcite peaks remains unchanged and a slight increase in the intensity of the HA peaks, indicating a change in the ratio of crystalline phases. The width of the diffuse halo becomes noticeably smaller, which may indicate the structuring of the amorphous phase (Fig. 1 *c*).

On the diffractogram of the sample aged for 28 days in SBF, only highly intense peaks of hydroxoapatite and low intensity peaks of calcite remain against the background of a more symmetrical diffuse halo (Fig. 1 *d*). That is, the glass becomes more structured with the inclusion of mainly one crystalline phase of HA.

La doping leads to slight changes in the crystal structure of HA, compared to undoped sol-gel glass (Fig. 2 *a*). More destruction of the crystalline structure of HA was observed when the sample was soaked in SBF for 7 and 14 days (Fig. 2 *b, c*). At the same time, a smaller amount of HA is formed and a significant amount of calcite is preserved (Fig. 2 *d*). Similarly to the undoped sample, the appearance of the vaterite

phase is recorded, the amount of which decreases after soaking in SBF for 14 days.

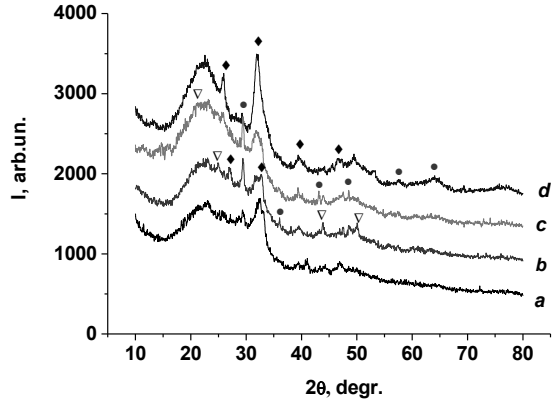

Fig. 1. XRD patterns of BG60S. *a* – before soaking in SBF solution, *b* – after 7 days, *c* – after 14 days, *d* – after 28 days soaking in SBF solution;
♦ – HA ($Ca_{10}(PO4)_6$ $(OH)_2$),
● – calcite ($CaCO_3$),
∇ – vaterite ($CaCO_3$)

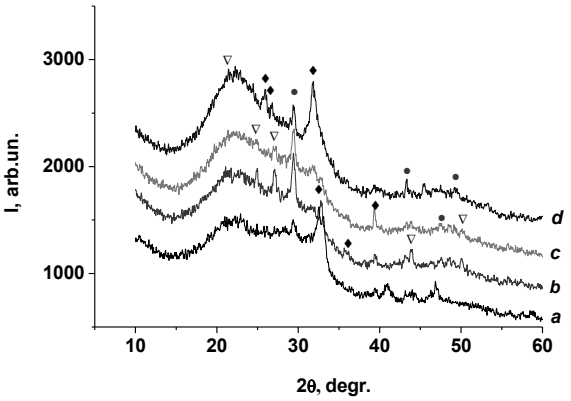

Fig. 2. XRD patterns of BG60S doped La. *a* – before soaking in SBF solution, *b* – after 7 days, *c* – after 14 days, *d* – after 28 days soaking in SBF solution;
♦ – HA ($Ca_{10}(PO_4)_6$ $(OH)_2$),
● – calcite ($CaCO_3$),
∇ – vaterite ($CaCO_3$)

Similarly to doped La 60S, Y doping causes a change in the crystal structure of HA (Fig. 3 *a*). Significant destruction of the NA structure and active formation of calcite was recorded after 7 days of soaking in SBF (Fig. 3 *b*). A trend of decreasing calcite/vaterite and increasing HA is observed for BG samples after 14 days and 28 days of soaking in SBF (Fig. 3 *c, d*).

EDX spectra of the samples show significant changes in the elemental composition of the surface after 7, 14 and 28 days of soaking in SBF. For BG60S (Table 1), the increase in the content of Ca and P with the simultaneous appearance of C is consistent with the formation of calcite (vaterite) phases on the surface and of the HA phase according to the data of XRD studies.

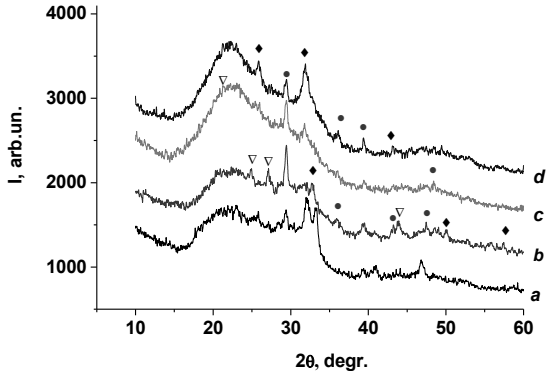

Fig. 3. XRD patterns of BG60S doped Y. *a* – before soaking in SBF solution, *b* – after 7 days, *c* – after 14 days, *d* – after 28 days soaking in SBF solution;
♦ – HA ($Ca_{10}(PO_4)_6$ $(OH)_2$),
● – calcite ($CaCO_3$),
∇ – vaterite ($CaCO_3$)

The BG60S doped La sample (Table 2) is characterized by a significantly smaller increase in P content, which is consistent with a lower HA content, according to the results of XRD studies. At the same time, the significant content of Ca and C on the surface of the samples after 7 and 14 days of soaking in SBF correlates with the presence of a calcite phase that persists after 28 days of soaking in SBF. A relative increase in the content of La may indicate the participation of this element in ion exchange processes and the formation of the HA phase.

The BG60S doped Y sample (Table 3) is characterized by the absence of C on the surface of the sample after 14 and 28 days of soaking in SBF, which may indicate a low content of the calcite phase on the surface of the sample. At the same time, the Ca/P ratio for this BG sample is 1:1.87 and 1:1.48 after 14 and 28 days of soaking in SBF, indicating the high crystallinity of the formed HA.

A decrease in the Si content is characteristic of all the studied samples. The presence of Na, Mg, Cl components of SBF is also recorded, which indicates active processes of ion exchange between the surface and SBF [25].

Table 1. EDX analyses of the samples BG60S before and after in SBF solution for 7, 14 and 28 days

Sample	O	Si	Ca	P	C	Mg	Na	Cl
before	52.6	27.8	15.6	4.1				
after 7	48.3	23.7	18.7	8.1		0.2	0.6	0.4
after 14	51.4	21.3	17.5	8.9	4.0	0.6	0.6	0.4
after 28	40.8	4.2	33.1	16.1	4.0	0.8	0.7	0.3

Table 2. EDX analyses of the samples BG60S doped La before and after in SBF solution for 7, 14 and 28 days

Sample	O	Si	Ca	La	P	C	Mg	Na	Cl
before	39.6	28.7	24.2	3.7	3.7				
after 7	35.2	18.6	23.8	4.3	12.3	4.5	0.5	0.4	0.4
after 14	37.2	10.4	24.7	7.9	13.2	4.8	0.7	0.7	0.9
after 28	43.8	12.8	16.9	7.8	9.8	7.2	0.5	0.6	0.6

Table 3. EDX analyses of the samples BG60S doped Y before and after in SBF solution for 7, 14 and 28 days

Sample	O	Si	Ca	Y	P	C	Mg	Na	Cl
before	50.3	27.2	15.0	3.4	4.2				
after 7	42.0	21.8	13.8	5.0	6.3	10.6		0.3	0.3
after 14	45.7	23.6	16.5	4.2	8.8			0.6	0.7
after 28	42.9	16.7	17.1	9.2	11.5		0.3	1.0	1.4

The obtained FTIR spectra of the synthesized BG samples showed changes in the surface composition before and after soaking in SBF solution and are presented in Figs. 4–6. According to the study, the synthesized bioactive glass has most of the characteristic maxima for silica mesh (Figs. 4–6). The maxima at 470, 800, and 1100 cm^{-1} are characteristic of the deformation vibration of Si–O–Si bridging bonds in SiO_4 tetrahedra, which have four oxygen atoms connected to four Si neighbors.

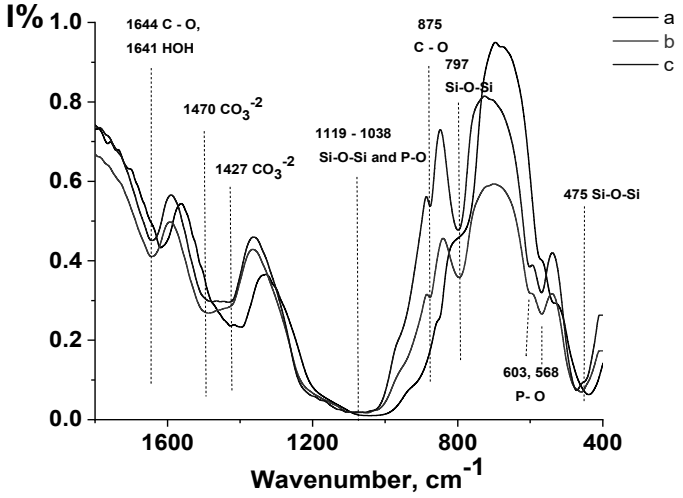

Fig. 4. FTIR-spectra of the sol-gel glass 60S: *a* – before immersion in SBF, *b* – after 7, *c* – after 14 days immersion in SBF

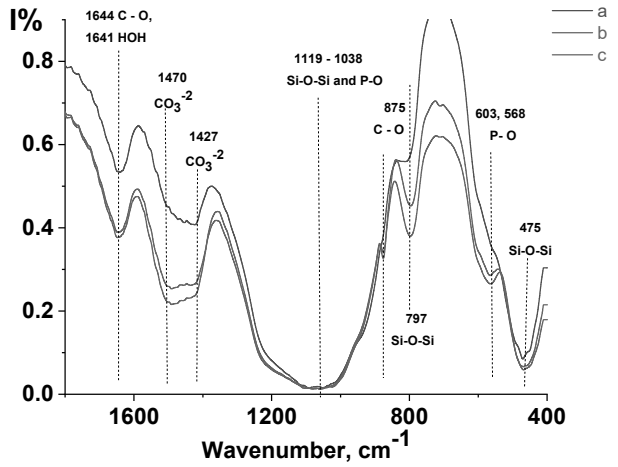

Fig. 5. FTIR -spectra of the sol-gel glass 60S doped La: *a* – before immersion in SBF, *b* – after 7, *c* – after 14 days soaking in SBF

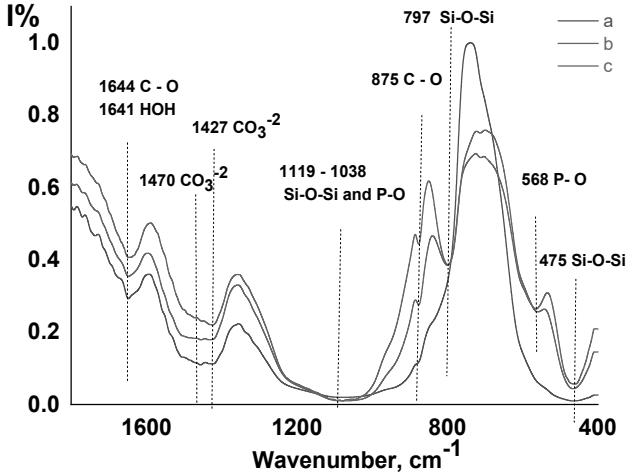

Fig. 6. FTIR-spectra of the sol-gel glass 60S doped Y: *a* – before immersion in SBF, *b* – after 7, *c* – after 14 days soaking in SBF

After immersion in the SBF solution (Figs. 4–6 *b, c*), the maxima characteristic of Si–O bonds at 800 cm^{-1} became much more intense. This confirms the formation of an amorphous surface layer rich in SiO_2 due to the dissolution of the vitreous network. The indistinct maximum at 1230 cm^{-1} refers to the symmetric and antisymmetric modes of Si–O–Ca bonds, which have non-bridging oxygen atoms.

In addition, after soaking in the SBF solution, two characteristic maxima appear at 570 and 605 cm^{-1}, which correspond to the deformation vibrations of the P–O bonds in the PO_4^{3-} group. Before immersion in SBF, their intensity is weak due to the small amount of phosphate bound to the glassy matrix. After immersion in the SBF solution (Figs. 4–6 *b, c*), these maxima become more intense, which may be associated with the active formation of both the amorphous and crystalline phases of HA. After 7 days of contact with SBF (Figs. 4–6 *b*), the increase in intensity at 1470 cm^{-1} and at 875 cm^{-1}, which is also recorded for the sample after 14 days (Figs. 4–6 *c*), is associated with active precipitation of the vaterite phase [26], which is consistent with the XRD data.

An increase in the intensity of the maxima at 1427 and 875 cm^{-1} and a change at 961 cm^{-1} after 14 days of immersion in SBF (Figs. 4–6 *c*) is associated with active $CaCO_3$ precipitation in the structure of the surface layer, which is consistent with XRD data.

This result, combined with XRD analysis and EDX data, confirms the bioactivity of the synthesized 60S bioactive glass samples.

CONCLUSIONS

EDX analysis confirms the presence of Si, Ca, P and La or Y (for doped samples). After 28 days of immersion in SBF, for the surface the predominant elements are Ca and P. The composition of the surface, shown by EDX, indicates that as a result of active ion exchange processes, the concentration of elements in the glass changes according to the theory of dissolution of bioactive glass in physiological fluids [27–29]. The increase in the concentration of Ca and P in the material is due to the formation of HA on the surface of the material.

The crystalline apatite layer aggregates and almost completely covers the glass surface for up to 28 days immersion in SBF solution, which leads to low detection of Si by EDX. It is believed that the formation of an apatite layer on the glass surface by biomineralization is an important step for the connection of glass with living tissue *in vivo*, the advantage of doped samples in the rate of formation of the HA layer correlates with research [30–32].

Detection of elements that are part of the model physiological fluid on the surface of the samples is a confirmation of active ion exchange processes occurring throughout the study period. It is necessary to note long and intensive processes involving CO_3^{2-} ions for undoped and doped La samples, which correlates with the results of FTIR - and XRD - studies. The formation of HA on the surface of the test specimens indicates that they are likely to have osteoconductive properties, may bind to bone tissue, and have a corresponding capability to biodegrade [33].

ACKNOWLEDGEMENT

This work was supported by the National Scholarship Programme of the Slovak Republic (ID 34575).

XRD, EDX та FTIR дослідження біоактивності скла 60S, легованого La та Y в умовах *in vitro*

А.П. Кусяк, О.І. Оранська, Д. Марцин Бегунова, А.Л. Петрановська, В.С. Чорний, О.А. Бур'янов, В.А. Дубок, П.П. Горбик

Інститут хімії поверхні ім. О.О. Чуйка Національної академії наук України
вул. Генерала Наумова, 17, Київ, 03164, Україна, a_kusyak@ukr.net
Інститут геотехніки Словацької академії наук
вул. Ватсонова, 45, Кошице, 04001, Словаччина
Національний медичний університет ім. О.О. Богомольця
бул. Тараса Шевченка, 13, Київ, 01601, Україна
Інститут проблем матеріалознавства ім. І.М. Францевича Національної академії наук України
вул. Кржижанівського, 3, Київ, 03142, Україна

Мета роботи – синтез та дослідження біоктивності в умовах in vitro зразків золь-гель скла (60S) мольного складу 60 % SiO_2, 36 % CaO, 4 % P_2O_5 та зразків, допованих La and Y, вивчення їхніх структурних властивостей та змін при контакті з модельним фізіологічним середовищем (SBF Kokubo's), а також встановлення можливості їх використання для тканинної регенерації та тканинної інженерії.

За результатами дослідження, взаємодія синтезованих зразків з SBF приводить до зміни фазового складу та співвідношення аморфної і кристалічних складових. Необхідно відзначити тривалі та інтенсивні процеси за участю іонів CO_3^{2-} для нелегованих і легованих зразків. Поява карбонату кальцію у формі ватериту при одночасному збільшенні вмісту кальциту є однією з ознак високої біоактивності синтезованих зразків. За результатами XRD, EDX та FTIR досліджень після 28 діб замочування в SBF, переважаючими елементами поверхні є Ca і P у складі гідроксиапатиту, а елементний склад свідчить про активні іонообмінні процеси відповідно до теорії розчинення біоактивного скла в фізіологічних рідинах.

Зміна співвідношення кристалічних фаз із включенням переважно однієї кристалічної фази гідроксоапатиту протягом 28 днів призводить до більшої структурованості поверхні синтезованих зразків

та вказує на те, що вони мають остеокондуктивні властивості, можуть зв'язуватися з кістковою тканиною та мають відповідну здатність до біодеградації.

Результати дослідження свідчать про перспективність синтезованих матеріалів для тканинної регенерації та тканинної інженерії.

***Ключові слова**: біоактивне золь-гель скло, остеокондуктивність, тканинна регенерація, тканинна інженерія*

REFERENCES

1. Fiume E., Migneco C., Kargozar S., Verné E., Baino F. Processing of Bioactive Glass Scaffolds for Bone Tissue Engineering. In: *Bioactive Glasses and Glass-Ceramics*. (eds Baino F., Kargozar S.). 2022.
2. Rahaman M.N., Day D.E., Sonny Bal B., Fu Q., Jung S.B., Bonewald L.F., Tomsia A.P. Bioactive glass in tissue engineering. *Acta Biomater*. 2011. **7**(6): 2355.
3. Deshmukh K., Kovářík T., Křenek T., Docheva D., Stich T., Pola J. Recent advances and future perspectives of sol–gel derived porous bioactive glasses: a review. *RSC Advances.* 2020. **10**(56): 33782.
4. Bramhill J., Ross S., Ross G. Bioactive Nanocomposites for Tissue Repair and Regeneration: a review. *Int. J. Environ. Res. Public Health.* 2017. **14**(1): 66.
5. Vallet-Regí M., Salinas A.J. 6 – Ceramics as bone repair materials. In: *Bone Repair Biomaterials*. Woodhead Publishing Series in Biomaterials. Second Edition. (Woodhead Publishing. 2019). P. 141.
6. Sugiura Y., Niitsu K., Saito Y., Endo T., Horie M. Inorganic process for wet silica-doping of calcium phosphate. *RSC Adv*. 2021. **11**(20):12330.
7. Wen C., Bai N., Luo L., Ye J., Zhan X., Zhang Y., Sa B. Structural behavior and in vitro bioactivity evaluation of hydroxyapatite-like bioactive glass based on the SiO_2-CaO-P_2O_5 system. *Ceram. Int.* 2021. **47**(13): 18094.
8. Fernandez de Grado G., Keller L., Idoux-Gillet Y., Wagner Q., Musset A.-M., Benkirane-Jessel N., Offner D. Bone substitutes: a review of their characteristics, clinical use, and perspectives for large bone defects management. *J. Tissue Eng*. 2018. **9**: 1.
9. Bianchi E., Vigani B., Viseras C., Ferrari F., Rossi S., Sandri G. Inorganic Nanomaterials in Tissue Engineering. *Pharmaceutics.* 2022. **14**(6): 1127.
10. Kaygili O., Keser S., Tatar C., Koytepe S., Ates T. Investigation of the structural and thermal properties of Y, Ag and Ce-assisted SiO_2-Na_2O-CaO-P_2O_5-based glasses derived by sol–gel method. *J. Therm. Anal. Calorim*. 2016. **128**(2) 765.
11. Fandzloch M., Bodylska W., Barszcz B., Trzcińska-Wencel J., Roszek K., Golińska P., Lukowiak A. Effect of ZnO on sol–gel glass properties toward (bio)application. *Polyhedron*. 2022. **223**: 1.
12. Awaid M., Cacciotti I. Bioactive Glasses with Antibacterial Properties: Mechanisms, Compositions and Applications. In: *Bioactive Glasses and Glass-Ceramics*. (John Wiley & Sons, Inc., 2022).
13. Sharifianjazi Fariborz, Parvin Nader, Tahriri Mohammadreza. Synthesis and characteristics of sol-gel bioactive SiO_2-P_2O_5-CaO-Ag_2O glasses. *J. Non-Cryst. Solids*. 2017. **476**: 108113.
14. Liu L., Pushalkar S., Saxena D., LeGeros R.Z., Zhang Y. Antibacterial property expressed by a novel calcium phosphate glass. *Journal of Biomedical Materials Research Part B: Applied Biomaterials*. 2013. **102**(3): 423.
15. Xia Li, Xiupeng Wang, Dannong He, Jianlin Shi. Synthesis and characterization of mesoporous CaO -MO-SiO_2-P_2O_5 (M = Mg, Zn, Cu) bioactive glasses/composites. *J. Mater. Chem.* 2008. **18**(34): 4103.
16. Simon V., Albon C., Simon S. Silver release from hydroxyapatite self-assembling calcium–phosphate glasses. *J. Non-Cryst. Solids.* 2008. **354**(15–16): 1751.
17. Giannoulatou V., Theodorou G.S., Zorba T., Kontonasaki E., Papadopoulou L., Kantiranis N., Chrissafis K., Zachariadis G., Paraskevopoulos K.M. Magnesium calcium silicate bioactive glass doped with copper ions; synthesis and *in-vitro* bioactivity characterization. *J. Non-Cryst. Solids.* 2018. **500**: 98.
18. Seyedmomeni Sh.S., Naeimi M., Raz M., Aghazadeh Mohandesi J., Moztarzadeh F., Baghbani F., Tahriri M. Synthesis, Characterization and Biological Evaluation of a New Sol-Gel Derived B and Zn-Containing Bioactive Glass: *In Vitro* Study. *Silicon.* 2018. **10**(2): 197.
19. Wren A.W., Jones M.C., Misture S.T., Coughlan A., Keenan N.L., Towler M.R., Hall M.M. A preliminary investigation into the structure, solubility and biocompatibility of solgel SiO_2-CaO-Ga_2O_3 glass-ceramics. *Mater. Chem. Phys*. 2014. **148**(1–2): 416.
20. Thanasrisuebwong P., Jones J.R., Eiamboonsert S., Ruangsawasdi N., Jirajariyavej B., Naruphontjirakul P. Zinc-Containing Sol-Gel Glass Nanoparticles to Deliver Therapeutic Ions. *J. Nanomater*. 2022. **12**(10): 1691.

21. Moonesi Rad R., Alshemary A.Z., Evis Z., Keskin D., Altunbaş K., Tezcaner A. Structural and biological assessment of boron doped bioactive glass nanoparticles for dental tissue applications. *Ceram. Int.* 2018. **44**(8): 9854.
22. Hamadouche M., Meunier A., Greenspan D.C., Blanchat C., Zhong J.P., La Torre G.P., Sedel L. Long-termin vivo bioactivity and degradability of bulk sol-gel bioactive glasses. *J. Biomed. Mater. Res.* 2000. **54**(4): 560.
23. Kokubo T., Takadama H. How useful is SBF in predicting in vivo bone bioactivity? *Biomaterials.* 2006. **27**(15): 2907.
24. Schröder R., Pohlit H., Schüler T., Panthöfer M., Unger R.E., Frey H., Tremel W. Transformation of vaterite nanoparticles to hydroxycarbonate apatite in a hydrogel scaffold: relevance to bone formation. *J. Mater. Chem. B.* 2015. **3**(35). 7079.
25. Kusyak A., Petranovska A., Dubok V., Chornyy V., Bur'yanov O., Korniichuk N., Gorbyk P. Adsorption immobilization of chemotherapeutic drug cisplatin on the surface of sol-gel bioglass 60S. *Funct. Mater*. 2021. **28**(1): 97.
26. Vagenas N. Quantitative analysis of synthetic calcium carbonate polymorphs using FT-IR spectroscopy. *Talanta*. 2003. **59**(4): 831.
27. Tilocca A., Cormack Alastair N. The initial stages of bioglass dissolution: a Car–Parrinello molecular-dynamics study of the glass-water interface. *Proceedings of the Royal Society A*. 2011. **467**: 2102.
28. Kusyak A., Dubok V., Chornyi V., Petranovska A., Gorbyk P., Abudayeh A. Features of biodegradation of sol-gel bioactive glass 60S doped with Ga, Ge. *Mol. Cryst. Liq. Cryst.* 2021. **719**(1): 29.
29. Buryanov O.A., Chornyi V.S., Dubok V.A., Savosko S. Reparative Regeneration by Substitution of Bone Tissue Defects with Bioglass, Using Regeneration Technologies. *Int. J. Morphol.* 2021. **39**(1): 186.
30. Neščáková Z., Kaňková H., Galusková D., Galusek D., Boccaccini A.R., Liverani L. Polymer (PCL) fibers with Zn-doped mesoporous bioactive glass nanoparticles for tissue regeneration. *Int. J. Appl. Glass Sci.* 2021. **12**(4): 588.
31. Kurtuldu F., Mutlu N., Michálek M., Zheng K., Masar M., Liverani L., Chen S., Galusek D., Boccaccini A.R. Cerium and gallium containing mesoporous bioactive glass nanoparticles for bone regeneration: Bioactivity, biocompatibility and antibacterial activity. *Mater. Sci. Eng. C.* 2021. **124**: 112050.
32. Wetzel R., Bartzok O., Brauer D.S. Influence of low amounts of zinc or magnesium substitution on ion release and apatite formation of Bioglass 45S5. *J. Mater. Sci.: Mater. Med.* 2020. **31**(10): 86.
33. Hench L. Bioceramics. *J. Am. Ceram. Soc.* 1998. **81**(7): 1705.

Received 31.08.2022, accepted 03.03.2023